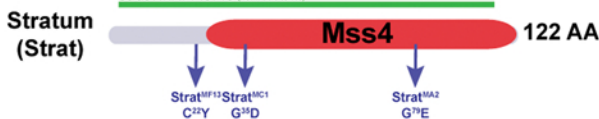


A

Strat RNAi v105730 (from AAR2 to 122)

Strat RNAi v45715 (from AAR3 to 115)



Alignment of Stratum and hMss4

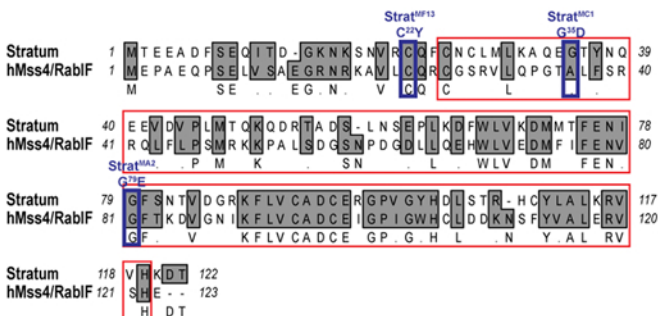
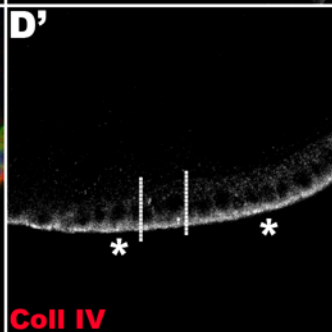
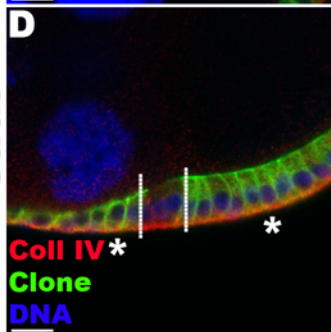
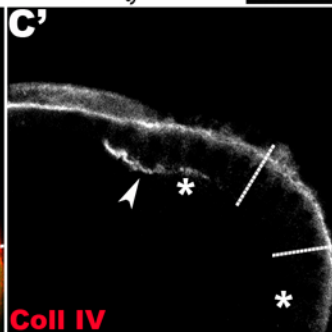
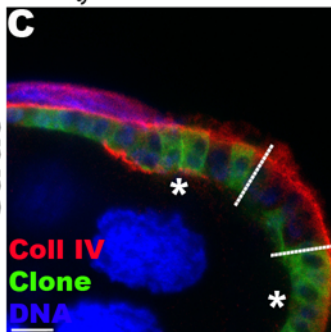
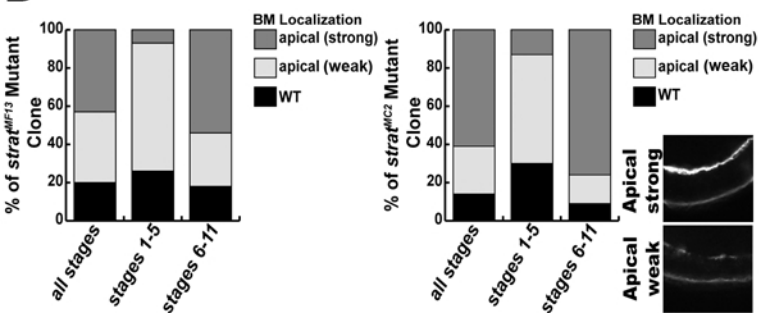
**B**

Figure S1. Generation of *stratum* mutant alleles. Related to Figure 1.

(A) Strat protein schematic and amino acid sequence alignment of *Drosophila* Strat and human Mss4 (hMss4/RabIF). Mss4 domain is in red. The *strat* mutations and the parts of the mRNA targeted by the two RNAi transgenes are indicated. The four mutants that we isolated fail to complement a deficiency uncovering the *strat* locus as well as each other, suggesting they belong to the same complementation group. The missense mutations identified in the newly isolated *strat* alleles are shown. For MF13 and MA2, mutations change conserved amino acids localized inside (MA2) or outside (MF13) of the Mss4 domain. (B) Quantification of the BM mislocalization phenotype observed in *strat*^{MF13} and *strat*^{MC2} mutant clones. Representative images are shown. A strong apical localization is observed more frequently in older egg chambers, indicating that secretion at the apical side is progressive during egg chamber maturation (C-D). Lg-sections through FC layers of egg chambers containing *strat*^{MC2} mutant clones (C) or *strat*^{MC2} mutant clones expressing Strat under control of UAS/Gal4 using the MARCM system (D). Clonal boundaries are indicated by dashed lines; and homozygous mutant FCs are indicated by asterisks (*) and the expression of the membrane marker mCD8-GFP (green). Egg chambers immunostained for α 1-Coll IV (red) and stained for DNA (blue). No apical accumulation of Coll IV is detected in *strat* mutant cells when Strat is expressed (D', compare to C'). This confirms that the BM deposition defect is due to mutation of *strat*. Thus, we successfully generated *strat* mutant alleles. Bars, 10 μ m.

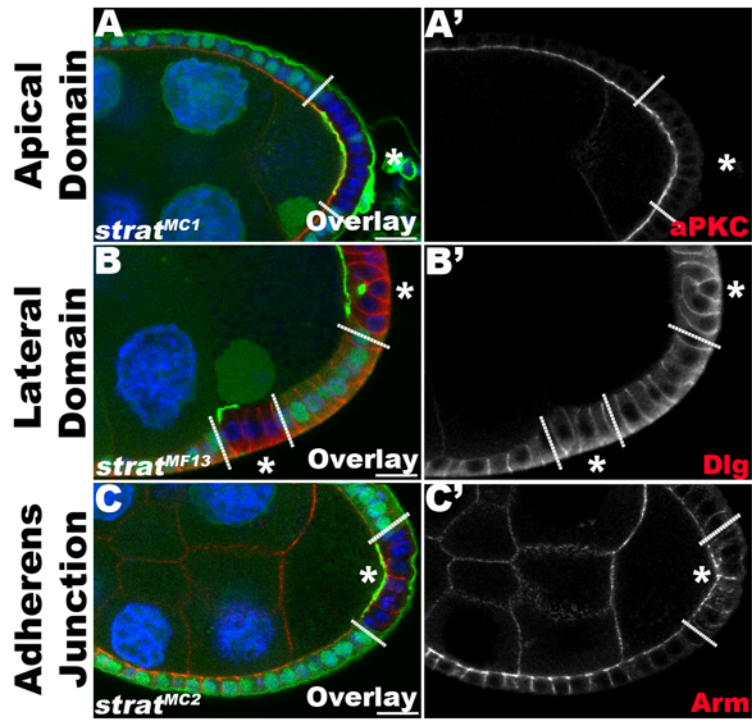
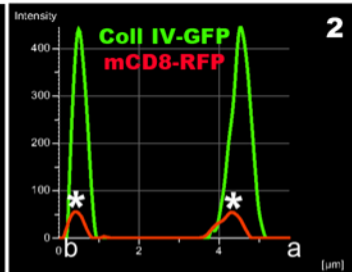
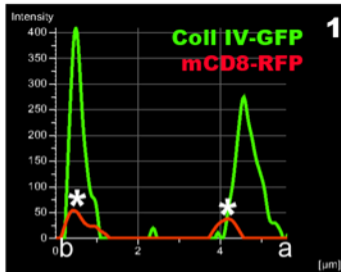
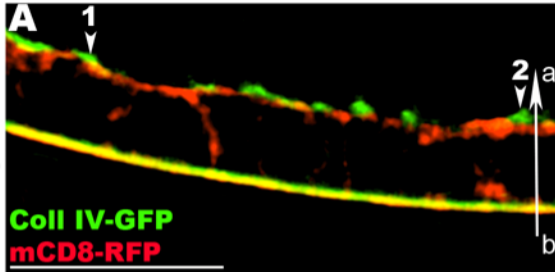


Figure S2. *stratum* mutant FCs maintain normal apical-basal polarity. Related to Figures 1 and 2.

(A-C) Lg-sections through FC layers of egg chambers containing *strat* mutant clones expressing Pcan-GFP (green). Clonal boundaries are indicated by dashed lines; homozygous mutant FCs are indicated by asterisks (*) and a loss of intracellular GFP (green). Egg chambers are immunostained for markers of epithelial polarity, including atypical Protein Kinase C (aPKC, A, red), Discs large (Dlg, B, red) and Armadillo (Arm, C, red), and stained for DNA (blue). *strat* mutant FCs do not show any differences in the distributions of the apical marker aPKC (A'), the lateral marker Dlg (B') or the adherens junction marker Arm (C'). Note the apical mislocalization of Pcan-GFP in *strat* mutant FCs (green, A-C). Altogether, these data indicate Strat is specifically required for restriction of BM deposition to the basal side of the cell. Bars, 10 μ m.

Crag RNAi



Crag RNAi

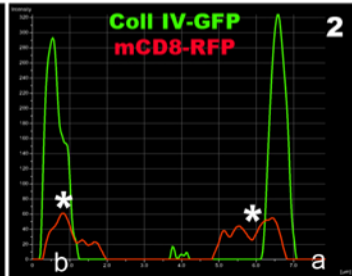
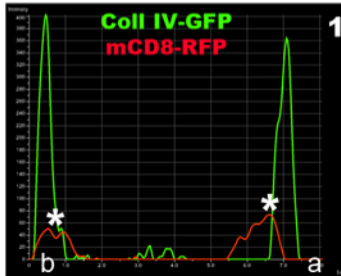
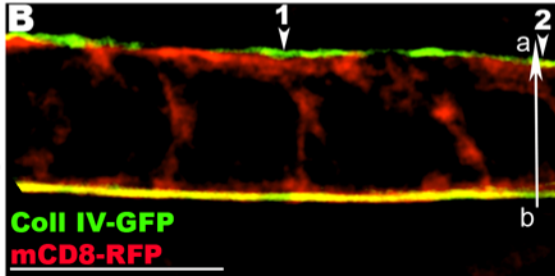


Figure S3. FCs depleted for *Crag* secrete apically BM proteins. Related to Figure 2.

(A-B) 3D-SIM reconstructions and micrographs of Lg-sections through *Crag* RNAi FE expressing Coll IV-GFP (green) and the membrane marker mCD8-RFP (red) exclusively expressed in the FCs. Histograms show the distributions of green (Coll IV-GFP) and red (mCD8-RFP) pixels along the basal-apical axis (b-a) at different positions of the epithelium (arrowheads). The *x*-axis represents the distance along the b-a axis (μm), while the *y*-axis represents arbitrary pixel intensity. The basal and apical plasma membranes are marked with asterisks (*). In *Crag* RNAi FCs, Coll IV accumulates both apically and basally in the FE. As shown by the micrographs and histograms, Coll IV and the plasma membrane are closely associated apically. However, Coll IV also accumulates apically outside of cells (green peaks are apical to red peaks). These data suggest that in *Crag* RNAi cells, as in *strat* RNAi cells (Figure 2), Coll IV is apically secreted outside of epithelial cells and stays associated with the plasma membrane. Bars, 10 μm .

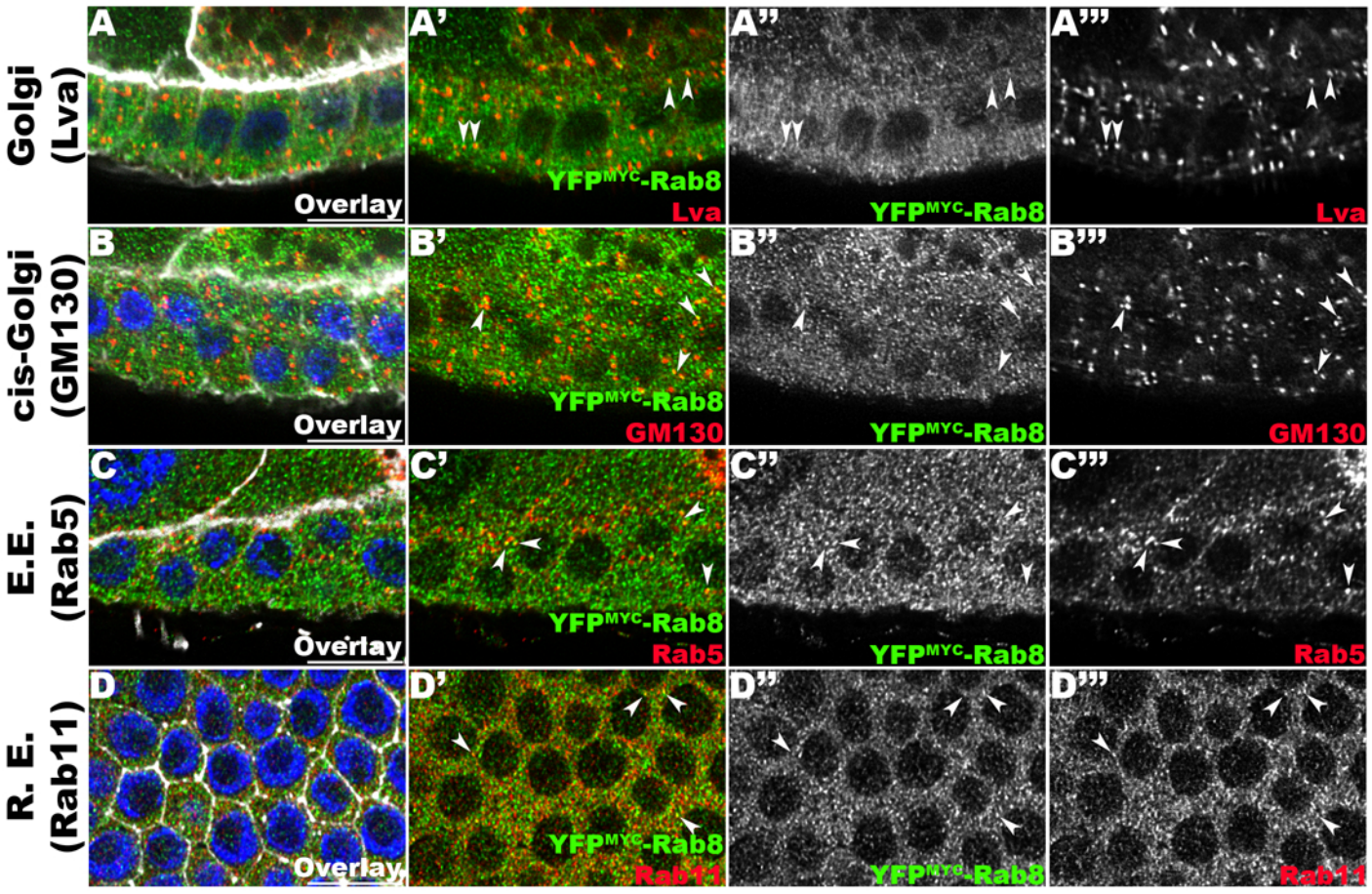


Figure S4. Subcellular distribution of Rab8 in the FE. Related to Figure 4.

(A-D) Lg-sections through egg chambers (Confocal ER) expressing an endogenously tagged YFP^{MYC}-Rab8 (green), stained for F-Actin (white), DNA (blue) and for the Golgi marker Lava lamp (Lva, A), a cis-Golgi marker (GM130, B), Rab5 (C) or Rab11 (D). Rab8 partially co-localizes with the Golgi (arrowheads, A' and B') and with the early endosome (E.E., Rab5, arrowheads, C') and the recycling endosome (R.E., Rab11, arrowheads, D'). Bars, 10 μ m.

Supplemental Experimental Procedures

Naming of CG7787

The basement membrane mislocalization phenotype observed in *CG7787* mutant cells is similar to the phenotype observed in *Crag* mutant cells. Thus, we chose a name for the gene *CG7787* emphasizing its relation to *Crag*, which in geology defines a steep rugged rock or cliff. Since BM proteins accumulate as a continuous apical sheet of BM proteins in *CG7787*-depleted epithelial cells, we named the gene *stratum* (*strat*), which defines a layer of sedimentary rock.

Additional antibodies used

The following additional primary antibodies were used: guinea pig anti-Coll IV α 1-chain (Cgc25c, 1:500, (Shahab et al., 2015)), rabbit anti-aPKC (1:1000, Santa Cruz), mouse anti-Armadillo (N2 7A1, 1:50, DSHB), mouse anti-Discs large (4F3, 1:100, DSHB), rabbit anti-Rab5 (1:50, (Wucherpennig et al., 2003)), rabbit anti-Rab11 (1:100, (Satoh et al., 2005)), rabbit anti Lava lamp (1:500, (Sisson et al., 2000)) and rabbit anti-GM130 (1:200, Abcam).

Generation of Crag Antibodies

For antibody production a fragment encoding aa 919–1666 of *Crag*-PA was used to generate rat anti-*Crag* polyclonal antibodies. The serum was used at 1:200 dilution for immunostaining.

Generation and isolation of mutant alleles of *stratum*

To generate *strat* mutant alleles, males of the genotypes *FRT40A cn* or *FRT40A cn bw* were mutagenized with EMS and their progeny tested using standard procedures (Chen and Schüpbach, 2006). To isolate *strat* mutant alleles, the potential mutants were mapped using different deficiency lines uncovering genomic regions around the *strat* locus: *Df(2L)BSC20* and *Df(2L)BSC229*, which both overlap with *strat*, and *Df(2L)ED578*, which does not overlap with *strat*. Deficiency lines used for mapping were obtained from the Bloomington Stock Center. We isolated four *strat* mutant alleles (*strat*^{MA2}, *strat*^{MC1}, *strat*^{MC2} and *strat*^{MF13}) that belong to the same complementation group. To identify the molecular lesions, each *strat* mutant line was balanced using *CyO*, *Kr::GFP* and genomic DNA from non-GFP-expressing *strat/strat* embryos was isolated. PCR products of the *strat* gene were sequenced and compared with those of *FRT40A* control products (Figure S1). Rescue of the BM proteins mislocalization phenotype observed in *strat* mutant FCs was performed by generating *strat* mutant cell clones that express UAS-Strat using the MARCM method (Lee and Luo, 1999) (Figure S1).

Molecular cloning and generation of transgenic lines

A full-length cDNA clone for *stratum* (clone #RE45155, Drosophila Genomics Resource Center) and a full-length cDNA clone for *hMss4/RabIF* (clone #4475846, GE Healthcare) were used as templates to generate transgenic lines. To generate *pUASp-strat* or *pUASp-hMss4*, the coding regions of *strat* or *hMss4*, respectively, were cloned into pTIGER, a derivative of the pUASp vector (Ferguson et al., 2012). To generate *pUASp-strat-HA*, the coding region of *strat* was cloned into pTIGER in frame with a C-terminal HA tag. These different constructs were inserted in the Drosophila genome via site-specific recombination (Φ C31 targeted integration (Markstein et al., 2008)) into attP40 (Chromosome II) and/or attP2 (Chromosome III) sites.

Co-Immunoprecipitation

The physical interaction between Strat and Rab8 was confirmed using ovary lysates expressing YFP^{MYC}-Rab8 under Rab8 endogenous promoter (Dunst et al., 2015) and/or Strat-HA using the UAS/Gal4 system. Ovaries were dissected in ice-cold PBS and homogenized in lysis buffer (50mM Tris pH 7.5, 100mM NaCl, 1mM EDTA, 1% NP40, protease inhibitor cocktail) using a pestle. Myc IP reactions were performed using anti-cMyc antibody (9E10, DSHB) and Protein A/G PLUS-Agarose beads (Santa Cruz) at 4°C for 2h. Total lysate and immunoprecipitates were separated via SDS-PAGE and analyzed by Western Blot using anti-

Myc (9E10, 1:100, DHSB) and anti-HA (3F10, 1:3000, Roche) antibodies followed by HRP-conjugated secondary antibodies (Jackson ImmunoResearch). Blots were imaged using a FluorChem HD2 system (Alpha Innotech).

Supplemental References

Chen, Y., and Schüpbach, T. (2006). The role of brinker in eggshell patterning. *Mech. Dev.* *123*, 395–406.

Ferguson, S.B., Blundon, M.A., Klovstad, M.S., and Schupbach, T. (2012). Modulation of gurken translation by insulin and TOR signaling in *Drosophila*. *J. Cell Sci.* *125*, 1407–1419.

Lee, T., and Luo, L. (1999). Mosaic Analysis with a Repressible Cell Marker for Studies of Gene Function in Neuronal Morphogenesis. *Neuron* *22*, 451–461.

Markstein, M., Pitsouli, C., Villalta, C., Celniker, S.E., and Perrimon, N. (2008). Exploiting position effects and the gypsy retrovirus insulator to engineer precisely expressed transgenes. *Nat. Genet.* *40*, 476–483.

Satoh, A.K., O'Tousa, J.E., Ozaki, K., and Ready, D.F. (2005). Rab11 mediates post-Golgi trafficking of rhodopsin to the photosensitive apical membrane of *Drosophila* photoreceptors. *Development* *132*, 1487–1497.

Sisson, J.C., Field, C., Ventura, R., Royou, A., and Sullivan, W. (2000). Lava Lamp, a Novel Peripheral Golgi Protein, Is Required for *Drosophila melanogaster* Cellularization. *J. Cell Biol.* *151*, 905–918.

Wucherpennig, T., Wilsch-Bräuninger, M., and González-Gaitán, M. (2003). Role of *Drosophila* Rab5 during endosomal trafficking at the synapse and evoked neurotransmitter release. *J. Cell Biol.* *161*, 609–624.